Ubiquitously expressed secretory carrier membrane proteins (SCAMPs) 1-4 mark different pathways and exhibit limited constitutive trafficking to and from the cell surface

Anna Castle* and David Castle

Department of Cell Biology, University of Virginia Health System, School of Medicine, Charlottesville, VA 22908, USA
*Author for correspondence (e-mail: amc3c@virginia.edu)

Accepted 17 May 2005
Journal of Cell Science 118, 3769-3780 Published by The Company of Biologists 2005
doi:10.1242/jcs.02503

Summary

Secretory carrier membrane proteins (SCAMPs) 1-4 are ubiquitously expressed and are major components of the eukaryotic cell surface recycling system. We investigated whether different SCAMPs function along distinct pathways and whether they behave like itinerant cargoes or less mobile trafficking machinery. In NRK cells, we show by immunofluorescence microscopy that different SCAMPs are concentrated mostly adjacent to one another in the trans-Golgi network and endosomal recycling compartment. By immunoelectron microscopy, they were shown to be close neighbors on individual transferrin-containing endosomal elements and on the plasma membrane. Within the internal endosomal network, SCAMPs are located distal to rab5-containing endosomes, and the individual isoforms appear to mark pathways that diverge from the constitutive recycling route and that may be distinguished by different adaptors, especially AP-1 and AP-3. Based on comparisons of SCAMP localization with endocytosed transferrin as well as live imaging of GFP-SCAMP1, we show that SCAMPs are concentrated within the motile population of early and recycling endosomes; however, they are not detected in newly formed transferrin-containing endocytic vesicles or in vesicles recycling transferrin to the surface. Also, they are not detected in constitutive secretory carriers marked by VSV-G. Their minimal recycling to the surface is reflected by their inability to relocate to the plasma membrane upon inhibition of endocytosis. Thus SCAMPs exhibit limited exchange between the cell surface and internal recycling systems, but within each of these sites, they form a mosaic with individual isoforms marking distinct pathways and potentially functioning as trafficking machinery at sites of vesicle formation and fusion. A corollary of these findings is that early endosomes exist as a distinct SCAMP-containing compartment and are not formed de novo by fusion of endocytic vesicles.

Supplementary material available online at
http://jcs.biologists.org/cgi/content/full/118/16/3769/DC1

Key words: SCAMPs, Membrane trafficking, Secretory carriers, Endocytosis

Introduction

Secretory carrier membrane proteins (SCAMPs) have been characterized as a family of integral membrane proteins with four transmembrane spans that are associated with regulated secretory carriers and with Golgi-derived and endosomal membranes (Brand and Castle, 1993; Brand et al., 1991; Brumell et al., 1995; Laurie et al., 1993). At least four distinct isoforms (SCAMP1-4) are ubiquitiously expressed in mammalian cells with a fifth isoform (SCAMP5) exhibiting primarily neural expression (Fernandez-Chacon and Sudhof, 2000b; Hubbard et al., 2000; Singleton et al., 1997). SCAMPs come in two sizes: ~38 kDa (SCAMP1-3) and ~25 kDa (SCAMP4 and 5). Topology studies of SCAMP1 have identified four closely spaced transmembrane spans that are flanked by amphipathic cytoplasmic segments, an organization that appears to be reiterated in the other SCAMPs (Hubbard et al., 2000). This core structure is conserved evolutionarily in the animal and plant kingdoms and is thought to be central to SCAMP function. Indeed, point mutations within the amphipathic cytoplasmic segment linking transmembrane spans 2/3 (E peptide) of SCAMP2 are known to have an inhibitory effect on late events in regulated exocytosis (Liu et al., 2002). SCAMP1-3 have extended N-terminal cytoplasmic segments that contain protein binding motifs that may regulate SCAMP function and intermolecular interactions (Brand and Castle, 1993; Fernandez-Chacon et al., 2000; Fernandez-Chacon and Sudhof, 2000b; Hubbard et al., 2000). Finally, the short, poorly exposed and unglycosylated ectoplasmic loops linking transmembrane spans 1/2 and 3/4 distinguish the SCAMPs from other four-span transmembrane proteins (e.g. tetraspanins, physins, MAL proteolipids, claudins, occludins, connexins and peripherin) that have extended hydrophilic and often glycosylated loops, which in many cases mediate intermolecular interactions (Anderson et al., 2004; Hemler, 2003; Hubner et al., 2002; Martin-Belmonte et al., 2003; Sohl and Willecke, 2004; Wrigley et al., 2000).

Recently, the localization and putative sites of SCAMP function have become increasingly complicated issues. Most of the earlier studies have emphasized the collective presence of SCAMPs in intracellular carriers involved in post-Golgi trafficking in many different cell types leading to the view that these carriers were the likely site of function (Brand and Castle, 1993; Brand et al., 1991; Brumell et al., 1995; Haass et al., 1996; Laurie et al., 1993; Laurie et al., 1992; Singleton et al., 1997; Wu and Castle, 1997). However, functional studies have suggested that SCAMP2 located in the plasma membrane rather than in the secretory granule supports exocytosis (Guo et al., 2002; Liu et al., 2002). The potential interaction of SCAMP1 with γ-synergin, an AP-1 adaptor-associated post-Golgi protein, and the prospective function of SCAMP1 in endocytosis (Fernandez-Chacon et al., 2000) implicate actions of SCAMPs at sites of vesicle formation. Thus it is unclear to what extent the association with vesicular carriers reflects a site of SCAMP function or SCAMPs in transit.

In the present study, we have used NRK cells to investigate whether SCAMP1-4 each have distinct localizations within constitutive recycling pathways. We have also examined their relationships to itinerant cargoes during membrane trafficking and upon perturbation by agents that interfere with trafficking. Our findings clearly delineate distinct distributions among different SCAMPs even within contiguous membrane surfaces. Quite surprisingly, they also reveal restricted movement of SCAMPs to and from the cell surface. These observations point to retention of SCAMPs at putative sites of vesicle formation and fusion and lead to new insights about the composition of endosomes and recycling vesicles.

Materials and Methods

Materials

Diaminobenzidene tetrahydrochloride, fish gelatin and most standard reagents were purchased from Sigma (St. Louis, MO) or Calbiochem (San Diego, CA). Antibodies used in this study were obtained as follows: syntaxin 6 (Stressgen, Victoria, British Columbia); TGN-38 mAb, gift of K. Howell, U. Colorado Health Science Center, Denver, CO; caveolin, γ-adaptin, σ3-adaptin (BD Biosciences, San Diego, CA); clathrin (X22 mAb) and transferrin receptor H68.4 mAb (ATCC, Rockville, MD); M6PR, gift of W. Brown, Cornell University, Ithaca, NY; CD63, gift of R. Siraganian, NIAID, NIH, Bethesda, MD; anti-Tac, gift of J. Donaldson, NICHD, NIH. Polyclonal SCAMP1 antibody 1α (Hubbard et al., 2000), SCAMP2 antibody 2τ (Liu et al., 2002), SCAMP3 antibody 3γ (Guo et al., 2002) and SCAMP4 antibody 4ω (Hubbard et al., 2000) were characterized previously. Alexa 488 and 594-conjugated antibodies were from Molecular Probes (Portland, OR).

cDNA constructs

For the GFP-SCAMP1 construct, rat SCAMP1 cDNA with a N-terminal myc tag (Liu et al., 2002) was subcloned into pEGFP-C1 vector (Clontech, BD Biosciences, San Diego, CA). Rab5 (in pGreen Lantern) and Rabs 4, 11 (in pEGFP-C3) were gifts of J. Casanova (University of Virginia); Tac in pXS was a gift of J. Donaldson (NICHD, NIH); ts045-EGFP-VSV-G was a gift of J. Lippincott-Schwartz (NICHD, NIH); GFP-tagged Eps15 lacking the DPF domain was a gift of A. Sorkin (University of Colorado Health Science Center).

Antibody coupling

Biotinylated SCAMP antibodies were prepared by binding antibody to Sulfolink resin (Pierce Endogen, Rockford, IL) conjugated to the epitope peptide (1 mg peptide per ml resin) and incubating with a five- to tenfold excess of sulfo-NHS-LC-biotin (100 mg/ml stock in DMSO; Pierce Endogen). The reaction was carried out according to the manufacturer's instructions and the antibody was eluted using 0.2 M glycine (pH 2.2) and neutralized. SCAMP antibody-colloidal gold conjugates were prepared by dialyzing affinity-purified antibodies into 2 mM sodium tetraborate, pH 8, concentrating to 300 μl (2 mg/ml) and mixing with 25 ml colloidal gold (5, 10, 15 nm) solutions (Ted Pella, Reading, PA) adjusted to the same pH with 0.25 M K_2CO_3. After 5 minutes, 100 μl of 5% carbowax (20 kDa in water) was added and the solutions were centrifuged for 45 minutes at 38,000 ***g***. The loose antibody-gold pellets were resuspended in PBS containing 0.2 mg/ml BSA, recentrifuged and resuspended in 2 ml of the same solution. For experiments, antibody-gold conjugates were centrifuged for 4 minutes at 2000 ***g*** to remove aggregates; supernatants were diluted in blocking solution and cleared again by centrifugation.

Cell lines and transfections

NRK cells and COS-7 cells were maintained in DMEM supplemented with 10% FBS, 100 U/ml penicillin and 100 μg/ml streptomycin. GFP-SCAMP1, GFP-VSVG and the Eps15 deletion mutant ΔDPF-GFP were transfected into cells using Lipofectamine-Plus (Invitrogen) according to the manufacturer's directions. Stable cell lines were selected using 0.4 mg/ml G418.

Immunofluorescence microscopy

NRK cells grown on glass coverslips were processed as described previously (Liu et al., 2002). In experiments with plasma membrane sheets, NRK cells plated on poly-D-lysine (50 μg/ml)-coated coverslips were sonicated (single pulse) in 25 mM HEPES, pH 7.0, 25 mM KCl, 2.5 mM magnesium acetate, 0.2 mM dithiothreitol (Hussain et al., 1999). Following sonication, the samples were briefly rinsed in the same solution, fixed and processed as for intact cells. Most images were collected in 0.3 μm stacks on a Zeiss microscope and were digitally deconvolved using OpenLab software (Improvision, Lexington, MA). Brightness and contrast of images was adjusted to enable visualization using Adobe Photoshop. Double immunolabeling with two rabbit antibodies was carried out by using one non-biotinylated and one biotinylated antibody. Staining with non-biotinylated antibody (and secondary antibody) was performed first followed by blocking with components A and B of a blocking kit for endogenous biotin (Molecular Probes). Subsequently, the samples were incubated with the biotinylated primary antibody followed by fluorescent neutravidin (Molecular Probes). For total internal reflection fluorescence microscopy (TIRF-M), cells were plated on glass bottom dishes, fixed, stained and viewed directly on an Olympus IX70 microscope fitted with a 60× PlanApo (1.45 NA oil objective) and modified for TIRF illumination.

Labeling with fluorescent ligands and antibodies

Cells on coverslips were preincubated for 1 hour in serum-free medium. To follow transferrin uptake, cells were chilled to 0°C on an ice-water slurry and incubated with 100 μg/ml Alexa 594-labeled transferrin (Molecular Probes) for 30-45 minutes. Cells were washed with cold DMEM and warmed to 37°C for the specified times. Samples were stripped of bound transferrin at low pH, fixed and immunolabeled as described above. To follow transferrin recycling to the surface, cells were incubated with 100 μg/ml Alexa 594-labeled transferrin for 10 minutes at 37°C and chased with DMEM containing 0.5 mg/ml unlabeled transferrin for 60 minutes. Colocalization of transferrin and SCAMP was estimated as described before (Liu et al.,

2002). Uptake of Texas Red-conjugated EGF (4 μg/ml) was performed as described for transferrin. Uptake of Tac antibody was performed as previously described (Naslavsky et al., 2003).

Live cell imaging

Cells were grown on glass bottom dishes and imaging was done in a CO_2-independent medium (Sigma, St Louis, MO). Time-lapse series were acquired on a Zeiss inverted microscope with a heated stage using a 100× oil immersion objective. Images from the red and green channels were acquired sequentially; therefore, merged images are slightly offset from each other in time. Exposure times were 0.3-0.5 second each, with a 0.1 second delay. Sequences were converted to QuickTime movies or individual frames were processed in Adobe Photoshop.

Immunoelectron microscopy of whole mounts and plasma membrane rip-offs

To visualize SCAMPs within the endosomal system by immunoEM, we followed a previous procedure (Stoorvogel et al., 1996). A431 cells were cultured on formvar-coated gold grids, loaded with transferrin-HRP (25 μg/ml) for 1 hour at 37°C, and incubated with diaminobenzidene (DAB) and hydrogen peroxide to stabilize transferrin-containing endosomes. After permeabilization with 0.5 mg/ml saponin and fixation with 1% formaldehyde (1 hour, 4°C), the samples were blocked sequentially with glycine and fish gelatin and labeled with primary anti-SCAMP antibodies (or purified rabbit IgG) conjugated to colloidal gold. Labeled specimens were washed, fixed in 1% glutaraldehyde, dehydrated in ethanol, critical point dried and carbon coated. Images were recorded with a digital camera, and gray levels were adjusted in Adobe Photoshop to increase visualization of gold particles above the density of the DAB-containing endosomes.

For immunolabeling of plasma membrane sheets, sparse cultures of NRK cells were chilled for 15 minutes at 4°C and washed once with cold PBS. Formvar-coated nickel grids coated with poly-D-lysine (300,000 kDa, 0.1% solution for 30 minutes) were applied to the chilled cells with slight pressure, then lifted upwards quickly and transferred to 2% formaldehyde, 0.1 M sodium phosphate for 15 minutes at room temperature. This procedure is a variation of that developed by Sanan and Anderson (Sanan and Anderson, 1991). Fixed specimens were washed with PBS, quenched with 20 mM glycine in PBS, and once in 5% BSA/5% goat serum in PBS (blocking buffer). Labeling was done with antibodies adsorbed to colloidal gold in blocking buffer containing 20 mM glycine overnight at 4°C. After rinsing in PBS, the grids were post-fixed with 4% glutaraldehyde/4% formaldehyde in 0.1 M sodium phosphate for 15 minutes and 2% osmium tetroxide in 0.1 M sodium cacodylate for 1 hour. Finally, they were washed in PBS, dipped in water, immersed for 30 minutes in 2% methylcellulose:uranyl acetate (9:1) on ice and drained to dryness on filter paper.

Results

SCAMP isoforms have similar distributions but they are distinct from one another

SCAMPs are abundant proteins in all types of mammalian cells examined to date (our unpublished findings). A previous study, which was conducted at relatively low resolution, suggested that SCAMP1-3 had distributions that were similar to each other (Singleton et al., 1997). The availability of good isoform-specific antibodies and improved methods for immunofluorescence analysis has enabled us to re-examine these distributions at higher resolution. The staining of each of the four SCAMPs was concentrated on perinuclear membranes (Fig. 1A-D). At higher resolution, we observed considerable overlap of SCAMP1 with SCAMP2 and 3 at perinuclear sites; however, there was less overlap at peripheral sites where yellow puncta were still observed but the relative abundance of distinct red and green puncta was increased (Fig. 1E,F). Interestingly, even in the perinuclear region, the overlap of isoforms was incomplete as neighboring red and green staining regions were readily visible (insets of Fig. 1E,F). Comparison of SCAMP1 and 4 (Fig. 1G and inset) showed almost completely distinct staining of these two isoforms whereas comparison of SCAMP2 and 3 showed moderate perinuclear overlap (less than in the case of SCAMP1 and 3) and almost no overlap peripherally (data not shown).

To clarify the spatial relationships among SCAMP1, 2 and 3, we compared their distributions at higher resolution using immunoelectron microscopy of permeabilized cells labeled with anti-SCAMP-gold conjugates (Fig. 2A-D). A431 cells were loaded with transferrin-HRP and the distributions of SCAMPs were examined on diaminobenzidene/H_2O_2-stabilized endosomes in whole mount preparations (Stoorvogel et al., 1996). As seen in images of triple-stained samples, SCAMP1-3 often appeared as clusters that were mostly

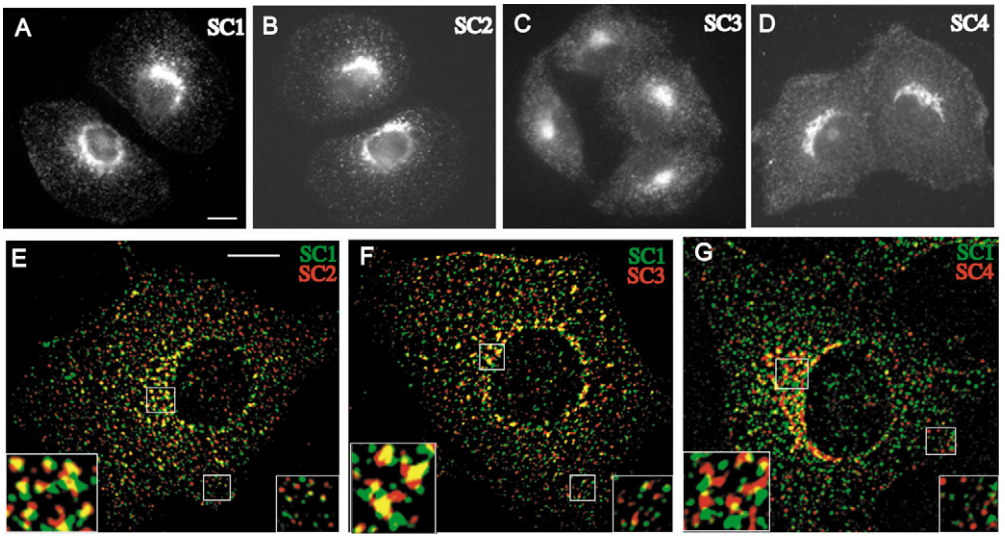

Fig. 1. Distribution of the four ubiquitously expressed mammalian SCAMPs in NRK cells. (A-D) low magnification wide-field images of SCAMP1-4 (SC1-SC4), emphasizing their concentration in perinuclear compartments. (E-G) Digitally deconvolved sections comparing the distribution of SCAMP1 to each of the other SCAMPs individually. SCAMP1 was detected using a biotinylated antibody 1α and SCAMP2 using 2τ, SCAMP3 using 3γ and SCAMP4 using 4ω. Insets at lower left illustrate the extent of overlap (yellow) at perinuclear sites while the insets at lower right are representative views showing limited overlap of isoforms in the peripheral cytoplasm. Bar, 10 μm.

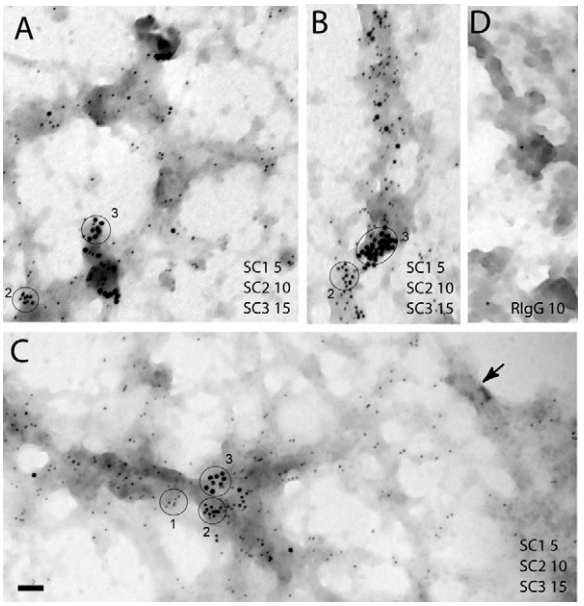

Fig. 2. Distribution of SCAMP1-3 on transferrin-loaded endosomes as viewed by immunoelectron microscopy on A431 cell whole mounts. (A-C) Examples of specimens stained for all three SCAMPs using primary antibody-gold conjugates: SCAMP1 (SC1), 5 nm gold; SCAMP2 (SC2), 10 nm gold; and SCAMP3 (SC3), 15 nm gold. The electron-dense areas represent HRP stain within endosomes. Clusters of SCAMP1, 2 and 3 are circled and numbered accordingly. The arrow in C identifies the plasma membrane and enables visualization of the absence of extracellular background staining. (D) Control specimen stained with affinity-purified rabbit IgG-10 nm gold at the same concentration used in the other samples. Bar, 100 nm.

isoform-specific within neighboring microdomains of individual transferrin-loaded endosomal structures (Fig. 2A-C). Clustering of SCAMP2 and 3 tended to be more extensive than for SCAMP1, which was often more dispersed. The labeling appeared similar in membranes located in the cell interior, but cell thickness precluded presenting easily visualized images. Staining with non-specific rabbit IgG-gold at the same concentration was negligible (Fig. 2D) and staining of low-density regions inside and outside cells was not noticeable (e.g. Fig. 2C). Thus we conclude that divergent distributions among different SCAMP isoforms are due in substantial part to segregation into domains of individual membrane surfaces.

Comparison of SCAMP distribution with markers of organelles

The predominant perinuclear accumulation of all four SCAMPs led us to compare their localizations to markers of organelles that are concentrated in this region of the cell. Cells were double labeled for individual SCAMPs and transferrin receptor (TfR), which is accumulated in the endosomal recycling compartment (ERC) (Fig. 3A-D). SCAMP1 showed the highest level of colocalization, especially in the larger staining foci whereas SCAMP2 and 3 showed moderate colocalization and SCAMP4 showed little colocalization except in selected more peripheral puncta. For EEA1, which concentrates on vesicular portions of early endosomes (Simonsen et al., 1998), we observed very limited colocalization with all four SCAMPs; where punctate structures exhibited green/red overlap, they appeared as neighbors (Fig. 3E-H). Interestingly, comparative staining of the SCAMPs and TGN-38, which is concentrated in the trans-Golgi network (TGN) (Ponnambalam et al., 1994), presented a picture that was nearly the converse of that observed for TfR. Here, SCAMP3 and especially SCAMP4 were significantly colocalized with TGN-38 whereas SCAMP1 and 2 showed little or no colocalization (Fig. 3I-L). We also examined SCAMP staining in relation to syntaxin 6, which is concentrated in a portion of the TGN and also accumulates in membranes that are in the vicinity of late endosomes (Bock et al., 1997). In this case, SCAMP1-3 exhibited substantial colocalization and SCAMP4 only limited colocalization (Fig. 3M-P). Finally, we localized the SCAMPs in relation to the mannose-6-phosphate receptor (M6PR) and the late endosomal/lysosomal marker CD63 (Rous et al., 2002). Overlap was limited in both cases (Fig. 3Q-T). Taken together, these comparisons extend earlier observations by showing that all the SCAMPs appear concentrated mainly in organelles involved in cell surface recycling rather than in organelles (including the EEA1-marked portion of early endosomes) that are linked to degradation (Brand and Castle, 1993; Brand et al., 1991). Also, they clarify that differences in localization among individual SCAMPs in the perinuclear region reflect at least partially their concentration in different organelles.

SCAMPs are associated with plasma membranes in NRK cells

The concentration of SCAMPs in compartments (TGN and ERC) that circulate membrane to the cell surface together with data implicating SCAMP1 in endocytosis (Fernandez-Chacon et al., 2000) and SCAMP1 and 2 in exocytosis (Fernandez-Chacon et al., 1999; Guo et al., 2002; Liu et al., 2002) suggested that SCAMPs should be present on plasma membranes. In order to address the presence of SCAMPs on the plasma membrane of NRK cells, we initially examined plasma membrane sheets prepared by brief sonication of cells attached to poly-D-lysine-coated coverslips and immunostained for individual SCAMPs and other marker proteins. All SCAMPs were readily detected on the plasma membranes where they appeared as discrete brightly or dimly stained puncta, illustrated for SCAMP1 and 2 (Fig. 4A,B). In all cases, the staining was very different from that of TfR, which exhibited a fairly smooth distribution across the whole surface (Fig. 4C). Staining for intracellular organelles, e.g. EEA-1 for early endosomes, was negligible indicating that the SCAMP foci were likely to have originated from sites within the cell surface (data not shown).

When the plasma membrane sheets were stained simultaneously for various combinations of two SCAMPs, we observed that there was only limited overlap, although puncta representing distinct SCAMPs were frequently close to one another. Neighboring SCAMPs were visualized by immunoEM on plasma membrane sheets ripped from the upper cell surface and labeled with primary antibodies directly conjugated to different sizes of colloidal gold. Fig. 4D shows that SCAMP staining was clearly within the plasma membrane surface and mainly appeared in clusters distinct from, but often closely apposed to clusters of a different SCAMP.

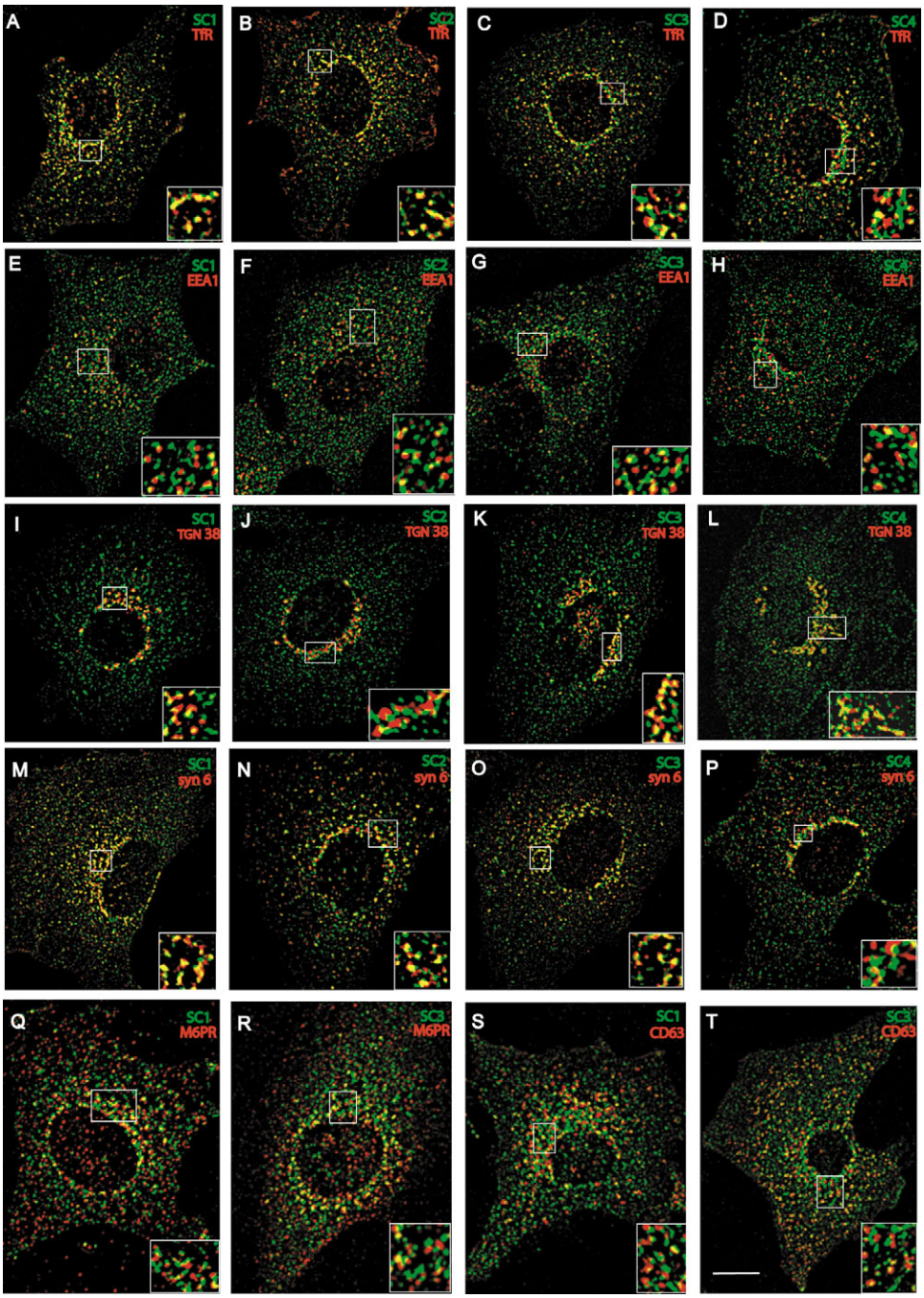

Fig. 3. Comparison of the distributions of each of the SCAMPs (SC1-SC4) to markers that localize to perinuclear and peripheral compartments in differing patterns. (A-D) Transferrin receptor (TfR), (E-H) EEA-1 (EEA1), (I-L) TGN-38 (TGN38) and (M-P) syntaxin 6 (syn6). SC1 and SC3 staining is also compared to mannose-6-phosphate receptor (M6PR) (Q,R) and to CD63 staining (CD63) (S,T). All images are digitally deconvolved sections, and the insets highlight differing degrees of overlap in the perinuclear region. Bar, 10 μm.

We also used plasma membrane sheets to compare the distributions of the SCAMPs with clathrin, adaptor AP-2 and dynamin 2. As illustrated for SCAMP1 and 2 (Fig. 4E-J), the SCAMPs mostly did not colocalize with these proteins although low levels of overlap were detected. This finding is consistent with the presence of SCAMPs at the perimeters, but mostly not within clathrin lattices seen by immunoEM (Fig. 4D, *).

We have attempted to identify other proteins that colocalize with SCAMPs on the plasma membrane, and to date, we have tested exocytotic t-SNAREs SNAP-23 and syntaxin 4, caveolin, phosphotyrosine-containing proteins, intersectin and tetraspanins CD9 and CD81. In no case have we observed significant codistribution with the surface foci (data not shown). Thus in contrast to that observed in regulated secretory cells where SCAMP2 overlaps in the plasma membrane with SNAP-23 and syntaxin 1 (Guo et al., 2002; Liu et al., 2002), we have not yet identified cell surface proteins in NRK cells with a substantially overlapping distribution.

SCAMPs are not detected in VSV-G-containing secretory carriers

SCAMPs appear partially or extensively colocalized with markers of the TGN (Fig. 2), and some of our previous studies have implicated SCAMPs as components of secretory carrier membranes. Thus we were interested whether they were detectable with cargo in constitutive secretory carriers in NRK cells. Cells were transfected with the ts045 mutant of GFP-tagged VSV-G protein, and a 20°C block was used to accumulate VSV-G in the TGN (Fig. 5A). The temperature was then increased to 32°C to permit VSV-G to exit the TGN in secretory vesicles. Tannic acid was added to inhibit exocytosis of the vesicles and allow their accumulation in the cytoplasm (Polishchuk et al., 2004). At 20°C, VSV-G extensively colocalized with SCAMP4 but not with other SCAMPs (Fig. 5B,C). Following warming in the presence of tannic acid, none of the SCAMPs was colocalized with VSV-G in the peripheral cytoplasm (Fig. 5E,F with SCAMP1 and 4 as examples) indicating that SCAMPs do not appear to travel in VSV-G containing constitutive secretory carriers. SCAMP4 also no longer colocalized with perinuclear VSV-G (Fig. 5F). Apparently residual VSV-G awaiting transport to the cell surface has separated from the SCAMP, providing a second

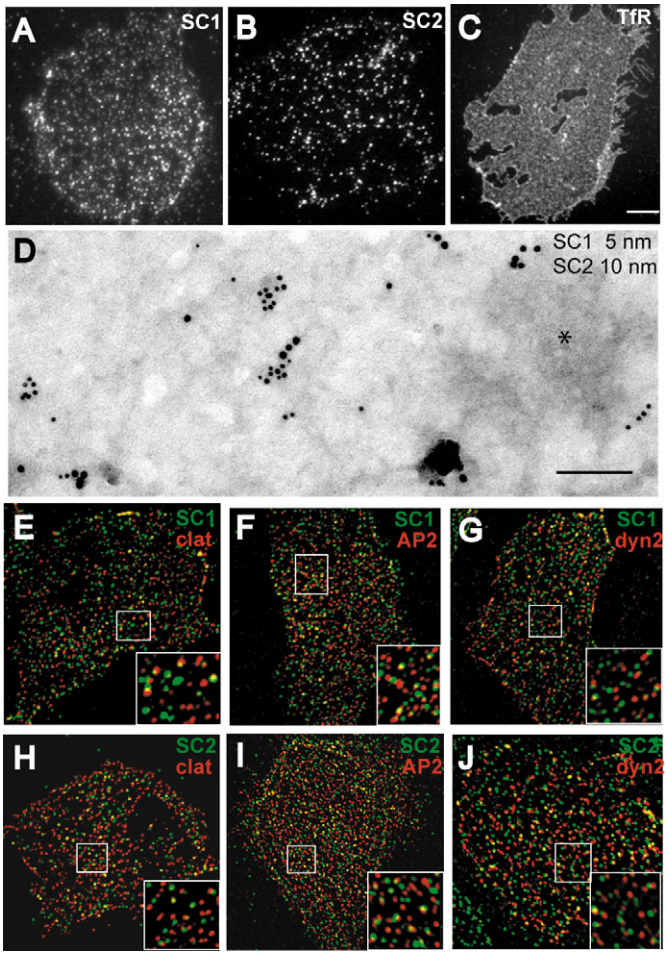

Fig. 4. SCAMPs on the plasma membrane. Plasma membrane sheets were labeled for SCAMP1 (A), SCAMP2 (B) or transferrin receptor (TfR) (C). (D) EM image of a portion of plasma membrane sheet ripped off the upper surface of an NRK cell and double labeled with antibodies against SCAMP1 and 2 conjugated directly to 5nm and 10 nm colloidal gold. Asterisk indicates clathrin-coated patch. Staining of SCAMP1 (E-G) and SCAMP2 (H-J) on plasma membrane sheets is also compared to clathrin (clat, E,H), adaptin AP2 (F,I) and dynamin 2 (dyn2, G,J). Insets illustrate limited colocalization. Bar, 10 μm (C); 100 nM (D).

level of distinction between the SCAMP and mobile cargo. The mechanism of this interesting shift in distribution is not known.

Localization of SCAMPs with endocytic tracers

Because the distinctions in SCAMP distribution were most apparent in the peripheral cytoplasm of NRK cells where early endosomes are located (Maxfield and McGraw, 2004), we explored whether endocytosed ligands would identify relationships between compartments marked by different SCAMPs. We began by examining the localization of SCAMP1-4 in relation to labeled transferrin, which is internalized by clathrin-mediated endocytosis and passes through the endosomal recycling system within 8-10 minutes of internalization (Maxfield and McGraw, 2004). Transferrin bound to cell surface receptors at 0°C was allowed to internalize at 37°C for various times, and its localization was compared to that of SCAMP1-4. In initial studies, we confirmed expeditious uptake of labeled transferrin followed by its concentration (Fig. 6A,B) and demonstrated early (within 10 seconds) association of transferrin with clathrin-coated pits and vesicles and subsequent uncoating by 20 seconds (Fig. 6C,D). At 20 seconds post uptake, none of the SCAMPs colocalized with transferrin (Fig. 6E-H). Strikingly, at 1 minute post uptake when punctate staining of transferrin in the peripheral cytoplasm was prominent (Fig. 6A), we observed extensive codistribution with all four SCAMPs, particularly SCAMP1 (Fig. 6I-L). When compared quantitatively with the individual SCAMPs, 75% of transferrin colocalized with SCAMP1-stained spots and 50%, 60% and 45% with SCAMP2, 3 and 4-stained spots, respectively. By 3 minutes when the internalized transferrin was mostly concentrated perinuclearly in the ERC, the corresponding staining for SCAMP1-4 (Fig. 6M-P) showed that colocalization with transferrin was extensive for SCAMP1 and SCAMP2 but was reduced for SCAMP3 and almost negligible for SCAMP4.

To evaluate the presence of SCAMPs in vesicles that return transferrin to the surface, we examined cells labeled with transferrin for 10 minutes and chased for an extended time (40-60 minutes). Transferrin punctate staining was generally separate from SCAMP staining, even for SCAMP1 and 2, which were colocalized at earlier times (Fig. 6Q-T). Taken together, these observations identify the majority of peripheral cytoplasmic SCAMP foci as part of the early endosomal network. Further, they imply that membranes internalizing transferrin from the surface may be relatively SCAMP-poor but rapidly fuse with existing endosomal membranes at sites that contain any of the four SCAMPs. Similarly, SCAMPs do not appear to be present in vesicles returning transferrin to the surface.

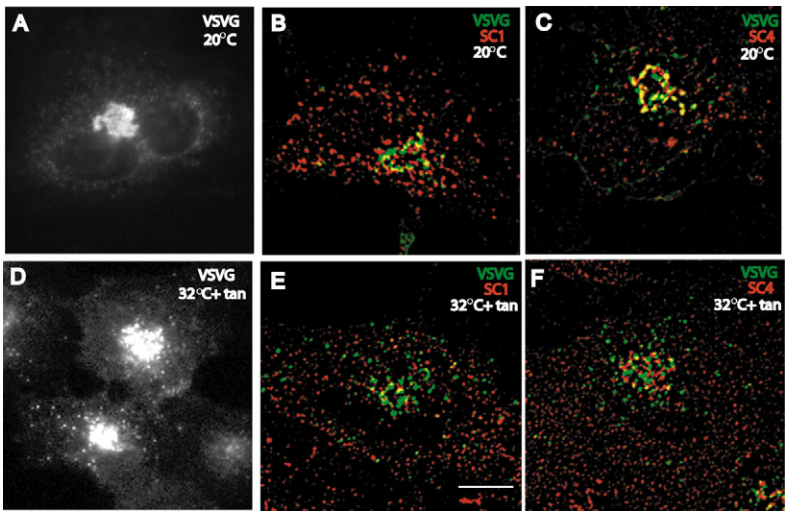

Fig. 5. SCAMPs are not detected in post-Golgi carriers for VSV-G. NRK cells transfected with GFP-VSVG were incubated at 39°C for 4 hours, then at 20°C for 2 hours to accumulate VSV-G in the TGN (A-C) and were warmed to 32°C for 30 minutes in the presence of 0.5% tannic acid to trap VSV-G in secretory carriers prevented from fusing with the plasma membrane (D-F). Deconvolved sections of cells immunostained for SCAMP1 (B,E) and SCAMP4 (C,F) compare the distributions of the SCAMPs to GFP-VSV-G. Bar, 10 μm.

We also compared the distributions of SCAMPs to internalized fluorescently tagged EGF. Examination at 3 and 15 minutes after uptake, corresponding to concentration of EGF with early sorting and late endosomal vesicles, respectively, indicated quite limited overlap of ligand with any of the SCAMPs, although the SCAMPs and EGF sometimes appeared as near neighbors (data not shown). This observation is consistent with an association of SCAMPs mainly with recycling pathways and not with pathways leading to late endosomes and ultimately lysosomes.

Finally, we examined whether SCAMPs were colocalized with the non-clathrin-mediated endocytic pathway that recycles Tac (the interleukin 2 receptor) and MHC1 complexes and is marked by internalization of anti-Tac antibody (Naslavsky et al., 2003). SCAMPs were detected at very low levels if at all in carriers containing endocytosed ligand when examined 5 minutes post uptake. However, appreciable colocalization with at least SCAMP1 was observed after 30 minutes of uptake (data not shown), consistent with the known intersection of the Tac pathway with the clathrin-mediated pathway (Naslavsky et al., 2003). Comparable findings concerning the absence of SCAMPs in the Tac recycling pathway have been obtained by Julie Donaldson (NICHD, NIH, Bethesda, MD).

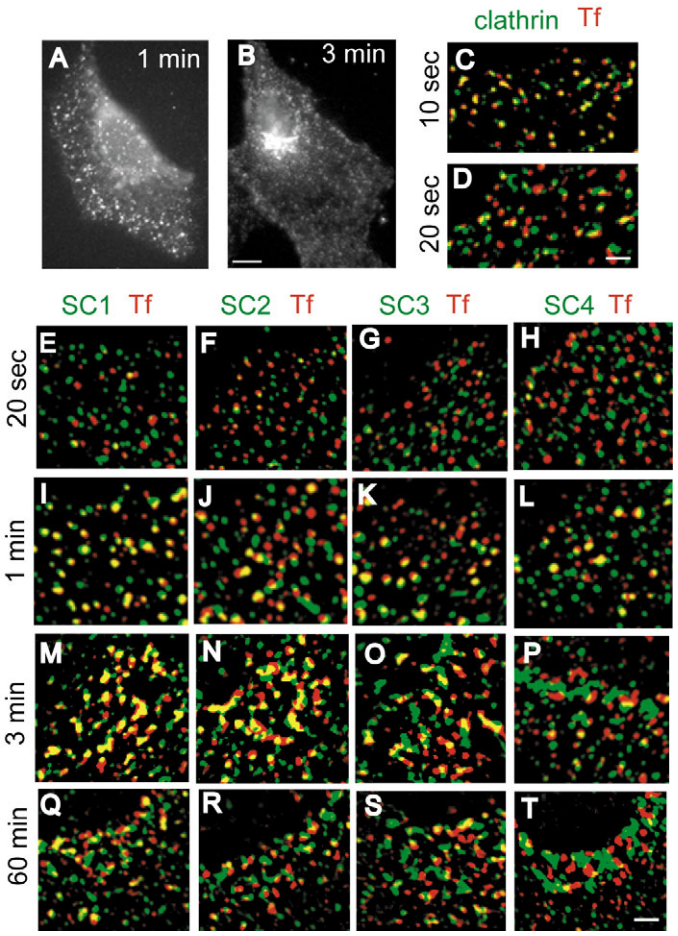

Fig. 6. Time course of fluorescent transferrin uptake and recycling and its association with SCAMP-containing compartments. (A-P) Alexa 594-transferrin (100 μg/ml) was bound to NRK cells at 0°C and uptake was initiated by warming to 37°C for the specified time. Whole cell images of uptake after 1 minute (A) and 3 minutes (B). (C,D) Deconvolved images 10 seconds (C) or 20 seconds (D) after uptake in cells stained for clathrin. (E-P) Deconvolved images comparing internalized transferrin at indicated times to the staining of SCAMP1-4. (E-I) portions of peripheral areas are shown. (M-P) portions of perinuclear areas are shown. (Q-T) To follow recycling carriers, cells were labeled with Alexa 594-transferrin for 10 minutes and chased for 60 minutes at 37°C. Deconvolved sections of perinuclear areas comparing transferrin and the staining of the SCAMPs are shown. Bar, 10 μm (B); 2 μm (D,T).

GFP-SCAMP1 mimics endogenous SCAMP1 and highlights distinctions in SCAMP and transferrin trafficking in fixed and live cell images

To begin addressing the dynamics of SCAMP trafficking and also to control for possible masking of endogenous SCAMP, we stably expressed an N-terminally tagged GFP-SCAMP1 chimera in NRK cells (~eightfold over endogenous SCAMP1) and compared its trafficking to endocytosed transferrin. In general, GFP-SCAMP1 exhibited a distribution that was very similar to that of endogenous SCAMP1 (Fig. 7A). Interestingly, however, we could readily detect colocalization of the tagged SCAMP with clathrin foci on plasma membrane sheets (Fig. 7B) in contrast to the limited colocalization observed for endogenous SCAMP and clathrin (Fig. 4). Even with the increased overlap, GFP-SCAMP1 was minimally colocalized with transferrin at 20 seconds post uptake whereas colocalization at 1 minute post uptake was extensive (Fig. 7C,D). These findings confirmed our previous suggestion that surface-derived vesicles are SCAMP-poor, and they fuse with membranes that are rich with resident SCAMPs.

For time-lapse video imaging of live cells, we initially examined events occurring shortly after a 10-minute transferrin labeling (emphasizing transferrin localization in early endosomes and the ERC). Extensive overlap of transferrin with GFP-SCAMP1 was observed within ~90 seconds (Fig. 7E). Supplementary material Movie 1 and extracted still frames (Fig. 7F) from recordings lasting 30 seconds showed that there were both stationary and mobile populations of labeled endosomes. In the stationary population, the fluorescent puncta oscillated back and forth around fixed positions whereas in the mobile population, the puncta underwent rapid saltatory movement. In all cases, SCAMP1 moved together with transferrin.

To examine the recycling pathway, we recorded events occurring after prolonged chase times (40-60 minutes) following transferrin labeling. Almost all the transferrin was segregated from GFP-SCAMP1-labeled endosomes (Fig. 7G). Transferrin was motile in vesicular and tubular profiles whereas SCAMP1 moved as separate puncta (Fig. 7H,I and supplementary material Movies 2, 3). Occasionally, we observed images where transferrin-labeled structures were attached to and tugging on SCAMP1-labeled puncta as if attempting to separate (supplementary material Movie 4 and Fig. 7J). These observations imply that just as for constitutive secretory carriers destined for the cell surface, constitutively recycling ERC-derived carriers lack detectable SCAMPs. Thus, the bulk of the SCAMP population appears to be within an intracellular membrane network and traffics minimally to and from the cell surface.

SCAMP distributions in cells expressing exogenous rab4, 5 and 11

In an effort to clarify how SCAMPs interface with the trafficking pathway of transferrin, we examined their distributions in cells overexpressing rab GTPases that regulate entry and recycling from early endosomes and the ERC. Thus we focused on rab4, 5 and 11, which form a mosaic of neighboring domains along this route (Sonnichsen et al., 2000), and we examined how endogenous SCAMPs were affected by overexpression of GFP-tagged chimeras of dominant inhibitory rabs (Fig. 8; examples in all cases shown for SCAMP1 and 4). Although wild-type rab5 localized near to all four SCAMPs in the peripheral cytoplasm, there was very little overlap with any of them (Fig. 8A,B). The proximity is best appreciated in the expanded vesicular early endosomes induced by overexpression of wild-type (and especially constitutively active) rab5 where the SCAMPs concentrate in foci (prospective tubular buds) peripheral to the central rab staining (Fig. 8A,B left insets). Overexpression of dominant-negative rab5-S35N had no obvious effect on the distribution of any of the SCAMPs (Fig. 8G-J), consistent with the limited presence of SCAMPs in internalized vesicles destined for rab5-mediated fusion with early endosomes.

In the case of rab4, we observed staining in close proximity to SCAMP1-3 but not SCAMP4 (Fig. 8C,D). For SCAMP1-3, expanded images (insets) show that overlap with rab4 is only partial suggesting that the SCAMPs congregate as close neighbors. Expression of dominant-negative rab4-I121N dispersed the perinuclear staining of SCAMP1 and 2 with little effect on SCAMP3 and no effect on SCAMP4 (Fig. 8K-N). These observations are consistent with the presence of SCAMP1-3 in rab4- and transferrin-positive tubules that exit early endosomes (Sonnichsen et al., 2000) (Fig. 7), whereas SCAMP4 labels a different endosome-derived pathway, possibly related to TGN trafficking. For rab 11, we observed staining significantly colocalized with all four SCAMPs (Fig. 8E,F), although overlap was only partial (insets), again suggesting that rabs and SCAMPs are neighbors. In this case, expression of the dominant-negative rab11-S25N resulted in reduced perinuclear staining and loss of larger stained structures for all SCAMPs (Fig. 8O-R) consistent with accumulation of all SCAMPs in either the ERC or TGN (Fig. 1) where functions of rab11 have been implicated (Ullrich et al., 1996; Wilcke et al., 2000).

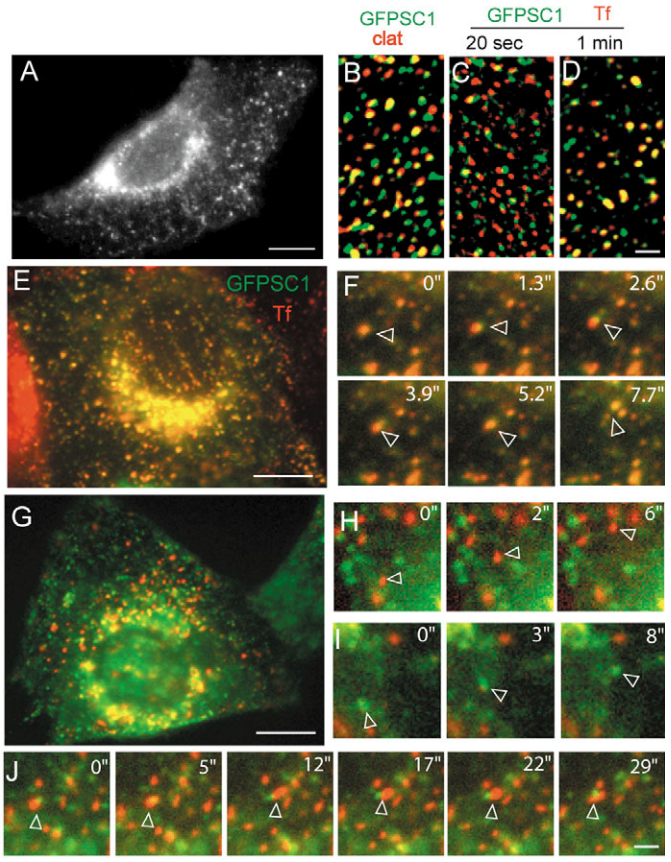

Fig. 7. Trafficking of transferrin in compartments marked by GFP-SCAMP1 at early and late times after uptake. (A) Overall image of a cell expressing GFP-SCAMP1. (B) Portion of a plasma membrane sheet from a GFP-SCAMP1 expressing cell labeled with anti-clathrin antibody (clat). (C,D) transferrin uptake in NRK cells stably expressing GFP-SCAMP1 was performed as in Fig. 6E-L and the internalization stopped after 20 seconds (C) and 1 minute (D). Cells were fixed and observed by fluorescence, and deconvolved sections are shown. (E,F) Cells expressing GFP-SCAMP1 were labeled for 10 minutes with Alexa 594-transferrin and chased for ~ 90 seconds. (E) Image of a live cell. (F) Selected frames from supplementary material Movie 1 of the cell shown in (E). The open arrowheads track the appearance (upper left panel) and movement of both transferrin and GFP-SCAMP1. The apparent separation of transferrin and GFP-SCAMP1 is due to sequential capture of images from the two different channels. (G-J) Live imaging of transferrin and GFP-SCAMP1 in carriers recycling transferrin to the surface. (G) Live cell expressing GFP-SCAMP1 imaged at 40 minutes of chase following a 15-minute labeling with Alexa 594-transferrin. (H) Selected images from Movie 2 in supplementary material showing transferrin movement (arrowhead) while GFP-SCAMP1 remains stationary. (I) Three panels from supplementary material Movie 3 showing movement of GFP-SCAMP1 (arrowhead) and not transferrin. (J) Selected images of supplementary material Movie 4 showing that distinct puncta of transferrin and GFP-SCAMP1 are tethered to one another and appear to be trying to separate during relocation (arrowhead). Bars, 10 μm (A,E,G); 2 μm (D,J).

SCAMP trafficking when clathrin-mediated endocytosis is inhibited

To provide independent confirmation of the apparent low level of trafficking of SCAMPs in constitutively recycling pathways, we examined whether inhibition of clathrin-mediated endocytosis elicited detectable changes in the steady-state distribution of the SCAMPs. COS-7 cells were used in place of NRK cells to achieve sufficient levels of transfection with a deletion mutant of Eps15 (ΔDPF-GFP), which selectively blocks clathrin-mediated endocytosis. Twenty-four hours after transfection, cells were either incubated with transferrin to assay its uptake or were fixed directly and immunostained for TfR or for each of the SCAMPs. Blockade of clathrin-mediated endocytosis in cells expressing ΔDPF-GFP (Fig. 9A,C) was confirmed by inhibition of transferrin uptake (not shown) and redistribution of TfR mostly to the plasma membrane (Fig. 9B). Interestingly, there was little or no detectable effect on the distribution of any of the SCAMPs; SCAMP1 is illustrated as an example (Fig. 9D). Both concentration in the ERC and presence in peripheral cytoplasmic foci appeared unaffected by

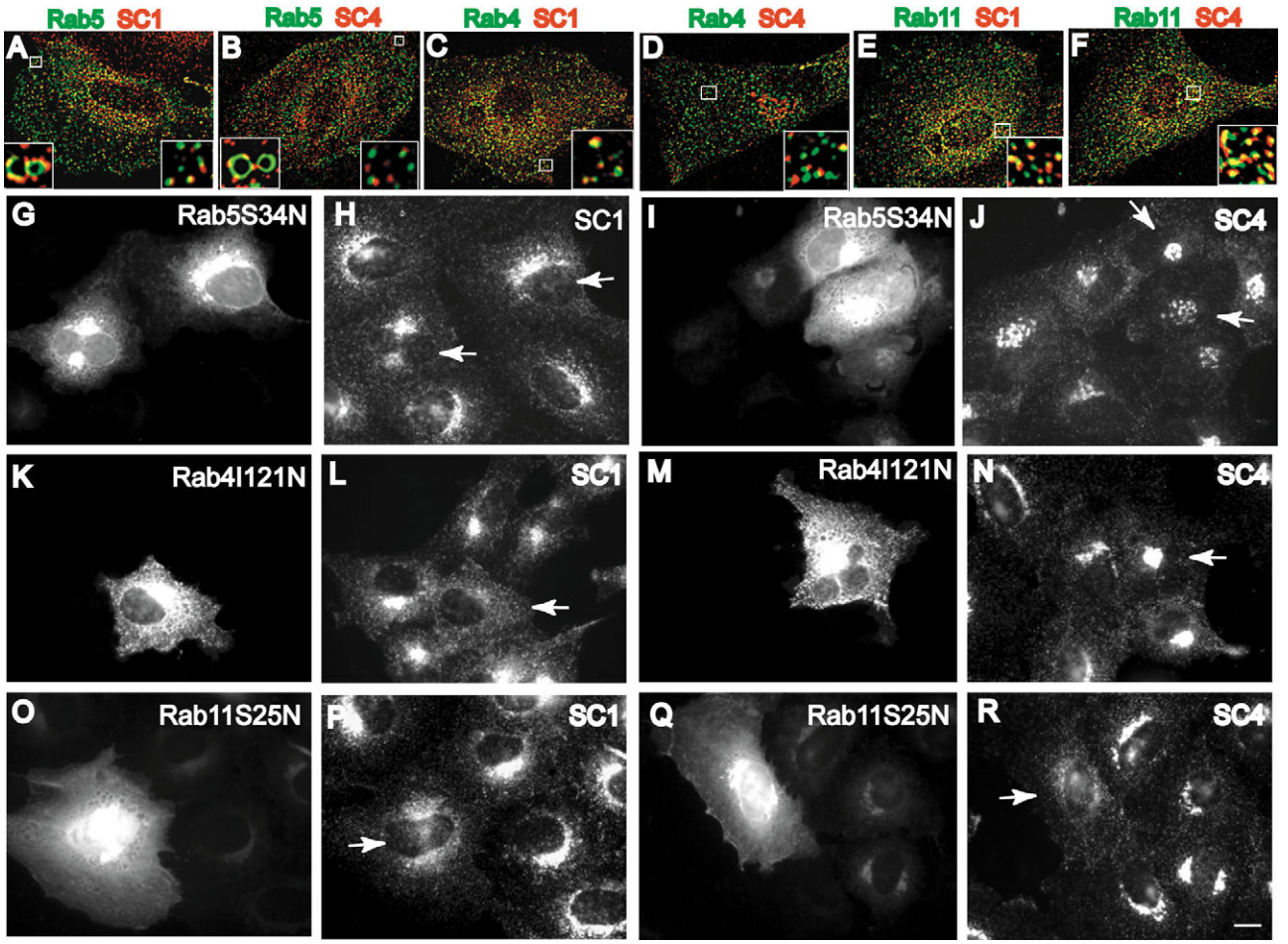

Fig. 8. Distribution of GFP-tagged Rabs 5, 4, and 11 in relation to endogenous SCAMPs illustrated using SC1 and SC4 as examples. (A-F) deconvolved images of cells expressing wild-type rabs: rab5 (A,B), rab4 (C,D) and rab11 (E,F) and stained for SCAMP1 (A,C,E) and SCAMP4 (B,D,F). Insets show extent of rab-SCAMP overlap at higher magnification from marked peripheral (A-D) and perinuclear (E,F) cytoplasmic regions. Left insets in A,B illustrate enlarged circular endosomal profiles typically observed in cells expressing rab5-Q67L with focal peripheral SCAMP staining. (G-R) Whole cell images of cells expressing GFP-tagged dominant-negative rab5-S34N (G-J), rab4-I121N (K-N) and rab11-S25N (O-R) and comparing GFP staining (G,I,K,M,O,Q) to SCAMP1 (H,L,P) and SCAMP4 (J,N,R). Cells expressing GFP-rab are indicated by arrows. Bar, 10 μm.

the endocytic block. To confirm the failure of SCAMPs to redistribute to the plasma membrane upon inhibiting endocytosis, we used total internal reflection fluorescence microscopy (TIRF-M). Cells expressing ΔDPF-GFP exhibited greatly increased surface TfR by TIRF-M whereas no change in SCAMP1 at the cell surface was detected (Fig. 9G-J).

No redistribution of any of the four SCAMPs has been detected in cells expressing dynamin mutant K44A, a broader spectrum inhibitor of post-Golgi recycling pathways (not shown). Similarly, cells treated with methyl-β-cyclodextrin exhibited no SCAMP redistribution (illustrated for SCAMP1 in Fig. 9E) even though redistribution of TfR was profound (Fig. 9F). We conclude that SCAMPs mainly travel intracellularly. Any larger-scale trafficking involving the cell surface may require specialized pathways.

SCAMPs 2 and 3 colocalize with AP-1 and AP-3 adaptor complexes

Because SCAMPs are concentrated at or near the TGN and in the ERC and also undergo changes in their extent of association with endocytosed transferrin, we were interested how SCAMP localization relates to the sites of sorting and formation of carrier vesicles. Consequently, we decided to examine their distribution in relation to adaptor complexes. SCAMP2 colocalized impressively with the AP-1 adaptor as marked by anti-γ-adaptin staining (Fig. 10A). Not only was codistribution observed at perinuclear (TGN/post-TGN) sites but it also extended throughout the peripheral cytoplasm suggesting that SCAMP2 marks endosomal sites where AP-1 mediated vesicular budding occurs (Deneka et al., 2003; Peden et al., 2004). SCAMP3 exhibited partial overlap with γ-adaptin mainly at perinuclear sites (Fig. 10B); however, it colocalized quite well, especially at perinuclear sites, with the AP-3 adaptor as marked by anti-σ3 staining (Fig. 10D). In other combinations of SCAMPs and adaptins, SCAMP1 overlap with γ-adaptin was similar to SCAMP3 while SCAMP4 overlap was limited (not shown); SCAMP1, 2 and 4 all exhibited limited overlap with σ3-adaptin (only SCAMP2 is shown in Fig. 10C).

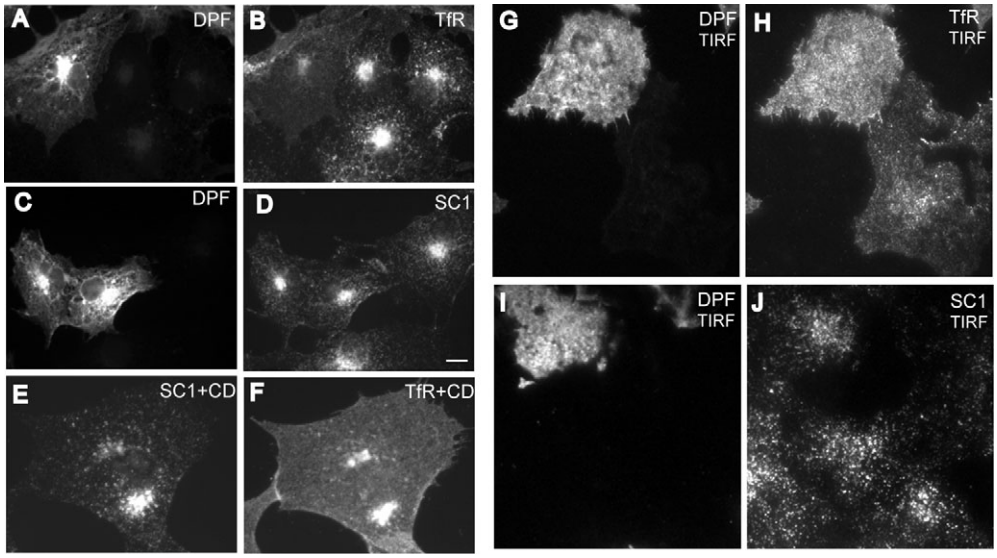

Fig. 9. The effect of Eps15-ΔDPF expression and of methyl-β-cyclodextrin on the distribution of constitutively recycling cargo and SCAMP1. COS-7 cells were transiently transfected with GFP-tagged Eps15-ΔDPF, fixed, immunostained for SCAMP1 or TfR and visualized by fluorescence (A-D) or TIRF-M (G-H) to compare SCAMP or TfR staining to GFP in paired images. (E,F) COS-7 cells were treated with 10 mM methyl-β-cyclodextrin (CD, 30 minutes, 37°C), fixed, double-labeled for SCAMP1 and TfR, and examined by fluorescence. Bar, 10 μm.

Discussion

Whereas our previous studies have mostly emphasized the distribution and function of selected SCAMPs in cells specialized for regulated secretion, the initial purpose of this study was to provide a detailed comparison of the distributions of the ubiquitously expressed SCAMP isoforms in a cultured mammalian cell type in order to gain potential insight as to how these abundant proteins are positioned to contribute to generic trafficking pathways. Although the steady-state distributions of individual SCAMPs were overtly similar to each other and emphasized association with post-Golgi surface recycling rather than degradative pathways, there were recognizable differences for each isoform with respect to sites of concentration and associations with selected markers of recycling routes. Indeed, in perinuclear compartments, all four SCAMPs exhibited accumulation and were colocalized to differing degrees with markers of the TGN, the ERC and one post-Golgi SNARE protein, syntaxin 6. At these sites and especially in peripheral early endosomes, it was also clear that the isoforms were close neighbors but mostly non-overlapping (Figs 1, 2). The same was true for the population of each SCAMP that we found in the plasma membrane (Fig. 4). Thus the individual SCAMPs form a non-overlapping mosaic of discrete domains throughout the recycling system and are accumulated in distinct territories within the major perinuclear recycling centers: the TGN and ERC.

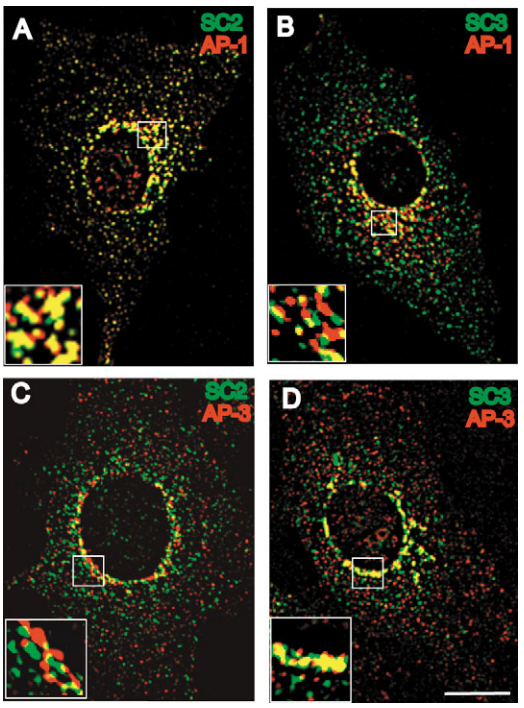

Fig. 10. Distribution of AP-1 and AP-3 adaptor complexes in relation to SCAMPs as viewed in deconvolved images of NRK cells. (A,B) Cells immunostained for AP-1 (γ-adaptin) and SCAMP2 (A) or SCAMP3 (B). (C,D) Cells immunostained for AP-3 (σ3) and SCAMP2 (C) or SCAMP3 (D). Insets in each panel highlight staining in the perinuclear region. Bar, 10 μm.

Several outcomes from the present study have led to new insight about where SCAMPs are located and what they might be doing. First, we were surprised that we did not detect SCAMP staining in constitutive secretory carriers, in newly internalized transferrin-containing vesicles after loss of their clathrin coats or in post-ERC carriers containing transferrin (Figs 5-7 and supplementary material, Movies 2-4). Further, the failure of SCAMPs to accumulate on the plasma membrane after inhibition of endocytosis (Fig. 9) implied that even rapidly recycling carriers (accounting for one-third to one-half of transferrin export) (Hao and Maxfield, 2000; Sheff et al., 1999) were likely to be SCAMP-poor. SCAMPs clearly do not behave as passive cargo; they are largely retained in internal membranes. Also SCAMPs on the plasma membrane tend to stay there even when overexpression increases colocalization with cell surface clathrin. Thus any circulation through the plasma membrane may represent either low-level leakage into constitutive pathways or export/import by specialized compensatory routes, e.g. regulated pathways as for SCAMPs in insulin-stimulated adipocytes (Laurie et al., 1993). The recently reported detection of SCAMPs in coated vesicles derived

from brain tissue (Blondeau et al., 2004) could reflect either of these possibilities.

The paucity of SCAMPs in newly internalized transferrin-containing vesicles yet the rapid appearance of transferrin in SCAMP-containing compartments was revealing from a second standpoint. It illustrates the distinct composition of integral membrane proteins in endosomes in relation to incoming vesicles, and it supports the concept that peripheral endosomes are an actual pre-existing compartment and not simply the product of homotypic fusion of newly uncoated vesicles generated by endocytosis. The existence of such a compartment has been difficult to evaluate because of its dynamic nature and limited volume (Maxfield and McGraw, 2004). SCAMP1 translocates with but eventually separates from passive cargo like transferrin (Fig. 7). Presumably, the SCAMP-containing membranes recycle, and if so, they almost certainly follow an intracellular route. It will be interesting to learn the fate of these SCAMP carriers and at what point they rejoin the pool of potential acceptor membranes for other rounds of fusion with imported vesicles.

The third notable realization was that all four SCAMPs mark peripheral early endosomes (labeled by transferrin at 1 minute) whereas upon appearance in the ERC, transferrin colocalized with only a subset of SCAMPs (Fig. 6I-P). Sustained and extensive colocalization of transferrin with SCAMP1 and 2, decreased colocalization with SCAMP3 and negligible association with SCAMP4 suggest that individual SCAMPs may separate into different pathways in the recycling network. This possibility is supported further by the clear differences in sites of high steady-state concentration among the SCAMP isoforms: SCAMP1 and 2 mainly in the ERC and SCAMPs 3 and 4 in the TGN. Separation along different transport routes may be facilitated by sequestering individual SCAMP isoforms in microdomains (Figs 2, 4).

Finally, the striking colocalization of at least two SCAMP isoforms with specific adaptor complexes and the detection of limited colocalization of all SCAMPs (and GFP-SCAMP1) with clathrin at the cell surface (Figs 4, 7) have led us to the interesting realization that foci of SCAMP staining may correspond in part to sites where carriers form within the recycling network. Although we do not yet have a comprehensive picture of whether the colocalization extends to other adaptors, the associations may signify a role of SCAMPs in vesicle nucleation. Bearing in mind that constitutive secretory carriers, newly uncoated endocytic vesicles, and post-ERC recycling carriers all are SCAMP-poor and that late endosomes, which are target organelles for AP-1 and AP-3 mediated traffic, are also not enriched in SCAMPs, we suspect that the SCAMPs may mostly remain at the sites where the vesicles bud. Thus in addition to the suspected functional roles of SCAMPs in facilitating membrane fusion during exocytosis (Fernandez-Chacon et al., 1999; Liu et al., 2002), it appears that SCAMPs may act in organizing membrane budding sites, potentially including sites that are weak and short-lived (Ehrlich et al., 2004). We envisage that similar vesicle fusion and bud organizing activities may be manifest throughout the recycling network. Evidently, these issues need to be examined directly.

Overall, our findings in NRK cells point to probable diversity among generic SCAMP isoforms with respect to which pathways they contribute during membrane trafficking. In this sense SCAMPs are like rab proteins, although our results (Fig. 8) clearly contrast the arrangements of SCAMPs and rabs to each other such that multiple SCAMPs are within pathway segments regulated by individual rabs and probably vice versa. In correlating SCAMP localization and potential functions with their structure, it seems likely that differences in sequences in N- and C-terminal cytoplasmic segments may determine their associations with particular pathways whereas the core of four transmembrane spans and conserved flanking sequences may impart both associations with membrane microdomains and a common action within the bilayer and at the cytoplasmic interface. Consequently, we regard the cytoplasmic N- and C-terminal segments as probable sources of individual localization signals and as sites responsible for prospective interactions with other trafficking machinery including intersectin, γ-synergin and the SNAREs (Fernandez-Chacon et al., 2000; Guo et al., 2002). The membrane core of one SCAMP, SCAMP2, has been implicated to function at a late step in exocytosis (Liu et al., 2002), and we presume that other SCAMPs have analogous roles at other sites of fusion and possibly at sites of vesicle fission. In view of recent observations that the most conserved segment (E peptide) within the SCAMP core sequesters acidic phospholipids, especially polyphosphoinositides (Ellena et al., 2004; Gambhir et al., 2004), one key activity may be to stabilize the lateral distribution of acidic phospholipids in territories that are conducive to fusion and formation of vesicles. Indeed many recent findings have documented the critical roles of polyphosphoinositides and their kinases and phosphatases in regulating these events (reviewed by Cremona and De Camilli, 2001; De Matteis and Godi, 2004). Finally, although we have now drawn distinctions among the different mammalian SCAMPs, we suspect for a few reasons that there may be overlap in their contributions to cell surface recycling activities. First, in mammalian neurons and in lower organisms (e.g. *Drosophila melanogaster*, *Caenorhabditis elegans*), more limited spectra of SCAMP isoforms (Fernandez-Chacon and Sudhof, 2000b; Hubbard et al., 2000; Singleton et al., 1997) are likely to support the full range of transport pathways. Second, mice in which SCAMP1 has been ablated appear able to conduct the full range of transport activities. Finally, both SCAMP1 and 2 have been implicated to function in regulated exocytosis of secretory granules in mast cells (Fernandez-Chacon et al., 1999; Guo et al., 2002). Just as there now appears to be functional redundancy between certain mammalian adaptor proteins (Traub, 2003), there may be redundancy between mammalian SCAMPs.

We thank Kathryn Howell, William Brown, Reuben Siraganian and Julie Donaldson for gifts of antibodies, Alexander Sorkin, Julie Donaldson, Jennifer Lippincott-Schwartz and Jim Casanova for cDNA constructs; Margaretta Allietta for conducting the immunoEM labeling and microscopy on plasma membranes; Claire Brown for guidance and assistance with TIRF-M and Lixia Liu for preparing the GFP-tagged SCAMP1 construct. We are grateful to Haini Liao and Jim Casanova for insightful comments on the manuscript. Studies were supported by a grant (DE09655) from the NIH.

References

Anderson, J. M., Van Itallie, C. M. and Fanning, A. S. (2004). Setting up a selective barrier at the apical junction complex. *Curr. Opin. Cell Biol.* **16**, 140-145.

Blondeau, F., Ritter, B., Allaire, P. D., Wasiak, S., Girard, M., Hussain, N. K., Angers, A., Legendre-Guillemin, V., Roy, L., Boismenu, D. et al. (2004). Tandem MS analysis of brain clathrin-coated vesicles reveals their critical involvement in synaptic vesicle recycling. *Proc. Natl. Acad. Sci. USA* **101**, 3833-3838.

Bock, J. B., Klumperman, J., Davanger, S. and Scheller, R. H. (1997). Syntaxin 6 functions in trans-Golgi network vesicle trafficking. *Mol. Biol. Cell* **8**, 1261-1271.

Brand, S. H. and Castle, J. D. (1993). SCAMP 37, a new marker within the general cell surface recycling system. *EMBO J.* **12**, 3753-3761.

Brand, S. H., Laurie, S. M., Mixon, M. B. and Castle, J. D. (1991). Secretory carrier membrane proteins 31-35 define a common protein composition among secretory carrier membranes. *J. Biol. Chem.* **266**, 18949-18957.

Brumell, J. H., Volchuk, A., Sengelov, H., Borregaard, N., Cieutat, A. M., Bainton, D. F., Grinstein, S. and Klip, A. (1995). Subcellular distribution of docking/fusion proteins in neutrophils, secretory cells with multiple exocytic compartments. *J. Immunol.* **155**, 5750-5759.

Cremona, O. and De Camilli, P. (2001). Phosphoinositides in membrane traffic at the synapse. *J. Cell Sci.* **114**, 1041-1042.

De Matteis, M. A. and Godi, A. (2004). PI-loting membrane traffic. *Nat. Cell Biol.* **6**, 487-492.

Deneka, M., Neeft, M., Popa, I., van Oort, M., Sprong, H., Oorschot, V., Klumperman, J., Schu, P. and van der Sluijs, P. (2003). Rabaptin-5alpha/rabaptin-4 serves as a linker between rab4 and gamma(1)-adaptin in membrane recycling from endosomes. *EMBO J.* **22**, 2645-2657.

Ehrlich, M., Boll, W., van Oijen, A., Hariharan, R., Chandran, K., Nibert, M. L. and Kirchhausen, T. (2004). Endocytosis by random initiation and stabilization of clathrin-coated pits. *Cell* **118**, 591-605.

Ellena, J. F., Malthroup, J., Wu, J., Rauch, M., Jayasinghe, S., Castle, J. D. and Cafiso, D. S. (2004). Membrane position of a basic aromatic peptide that sequesters phosphatidylinositol 4,5 bisphosphate determined by site-directed spin labeling and high resolution NMR. *Biophys. J.* **87**, 3221-3233.

Fernandez-Chacon, R. and Sudhof, T. C. (2000b). Novel SCAMPs lacking NPF repeats: Ubiquitous and synaptic vesicle-specific forms implicate SCAMPs in multiple membrane-trafficking functions. *J. Neurosci.* **20**, 7941-7950.

Fernandez-Chacon, R., Toledo, G. A., Hammer, R. E. and Sudhof, T. C. (1999). Analysis of SCAMP1 function in secretory vesicle exocytosis by means of gene targeting in mice. *J. Biol. Chem.* **274**, 32551-32554.

Fernandez-Chacon, R., Achiriloaie, M., Janz, R., Albanesi, J. P. and Sudhof, T. C. (2000). SCAMP1 function in endocytosis. *J. Biol. Chem.* **275**, 12752-12756.

Gambhir, A., Hangyas-Mihalyne, G., Zaitseva, I., Cafiso, D. S., Wang, J., Murray, D., Pentyala, S. N., Smith, S. O. and McLaughlin, S. (2004). Electrostatic sequestration of PIP2 on phospholipid membranes by basic/aromatic regions of proteins. *Biophys. J.* **86**, 2188-2207.

Guo, Z., Liu, L., Cafiso, D. and Castle, D. (2002). Perturbation of a very late step of regulated exocytosis by a secretory carrier membrane protein (SCAMP2)-derived peptide. *J. Biol. Chem.* **277**, 35357-35363.

Haass, N. K., Kartenbeck, M. A. and Leube, R. E. (1996). Pantophysin is a ubiquitously expressed synaptophysin homologue and defines constitutive transport vesicles. *J. Cell Biol.* **134**, 731-746.

Hao, M. and Maxfield, F. R. (2000). Characterization of rapid membrane internalization and recycling. *J. Biol. Chem.* **275**, 15279-15286.

Hemler, M. E. (2003). Tetraspanin proteins mediate cellular penetration, invasion, and fusion events and define a novel type of membrane microdomain. *Annu. Rev. Cell Dev. Biol.* **19**, 397-422.

Hubbard, C., Singleton, D., Rauch, M., Jayasinghe, S., Cafiso, D. and Castle, D. (2000). The secretory carrier membrane protein family: Structure and membrane topology. *Mol. Biol. Cell* **11**, 2933-2947.

Hubner, K., Windoffer, R., Hutter, H. and Leube, R. E. (2002). Tetraspan vesicle membrane proteins: synthesis, subcellular localization, and functional properties. *Int. Rev. Cytol.* **214**, 103-159.

Hussain, N. K., Yamabhai, M., Ramjaun, A. R., Guy, A. M., Baranes, D., O'Bryan, J. P., Der, C. J., Kay, B. K. and McPherson, P. S. (1999). Splice variants of intersectin are components of the endocytic machinery in neurons and nonneuronal cells. *J. Biol. Chem.* **274**, 15671-15677.

Laurie, S. M., Mixon, M. B., Brand, S. H. and Castle, J. D. (1992). A secretion granule membrane protein (GRAMP 92) is found in non-granule membranes including those of the endocytic pathway. *Eur. J. Cell Biol.* **58**, 12-27.

Laurie, S. M., Cain, C. C., Lienhard, G. E. and Castle, J. D. (1993). The glucose transporter GluT4 and secretory carrier membrane proteins (SCAMPs) colocalize in rat adipocytes and partially segregate during insulin stimulation. *J. Biol. Chem.* **268**, 19110-19117.

Liu, L., Guo, Z., Tieu, Q., Castle, A. and Castle, D. (2002). Role of secretory carrier membrane protein SCAMP2 in granule exocytosis. *Mol. Biol. Cell* **13**, 4266-4278.

Martin-Belmonte, F., Martinez-Menarguez, J. A., Aranda, J. F., Ballesta, J., de Marco, M. C. and Alonso, M. A. (2003). MAL regulates clathrin-mediated endocytosis at the apical surface of Madin-Darby canine kidney cells. *J. Cell Biol.* **163**, 155-164.

Maxfield, F. R. and McGraw, T. E. (2004). Endocytic recycling. *Nat. Rev. Mol. Cell Biol.* **5**, 121-132.

Naslavsky, N., Weigert, R. and Donaldson, J. G. (2003). Convergence of non-clathrin- and clathrin-derived endosomes involves Arf6 inactivation and changes in phosphoinositides. *Mol. Biol. Cell* **14**, 417-431.

Peden, A. A., Oorschot, V., Hesser, B. A., Austin, C. D., Scheller, R. H. and Klumperman, J. (2004). Localization of the AP-3 adaptor complex defines a novel endosomal exit site for lysosomal membrane proteins. *J. Cell Biol.* **164**, 1065-1076.

Polishchuk, R., Di Pentima, A. and Lippincott-Schwartz, J. (2004). Delivery of raft-associated, GPI-anchored proteins to the apical surface of polarized MDCK cells by a transcytotic pathway. *Nat. Cell Biol.* **6**, 297-307.

Ponnambalam, S., Rabouille, C., Luzio, J. P. and Nilsson, T. (1994). The TGN38 glycoprotein contains two non-overlapping signals that mediate localization to the trans-Golgi network. *J. Cell Biol.* **125**, 253-268.

Rous, B. A., Reaves, B. J., Ihrke, G., Briggs, J. A., Gray, S. R., Stephens, D. J., Banting, G. and Luzio, J. P. (2002). Role of adaptor complex AP-3 in targeting wild-type and mutated CD63 to lysosomes. *Mol. Biol. Cell* **13**, 1071-1082.

Sanan, D. A. and Anderson, R. G. (1991). Simultaneous visualization of LDL receptor distribution and clathrin lattices on membranes torn from the upper surface of cultured cells. *J. Histochem. Cytochem.* **39**, 1017-1024.

Sheff, D. R., Daro, E. A., Hull, M. and Mellman, I. (1999). The receptor recycling pathway contains two distinct populations of early endosomes with different sorting functions. *J. Cell Biol.* **145**, 123-139.

Simonsen, A., Lippe, R., Christoforidis, S., Gaullier, J. M., Brech, A., Callaghan, J., Toh, B. H., Murphy, C., Zerial, M. and Stenmark, H. (1998). EEA1 links PI(3)K function to Rab5 regulation of endosome fusion [see comments]. *Nature* **394**, 494-498.

Singleton, D. R., Wu, T. T. and Castle, J. D. (1997). Three mammalian SCAMPs (secretory carrier membrane proteins) are highly related products of distinct genes having similar subcellular distributions. *J. Cell Sci.* **110**, 2099-2107.

Sohl, G. and Willecke, K. (2004). Gap junctions and the connexin protein family. *Cardiovasc. Res.* **62**, 228-232.

Sonnichsen, B., De Renzis, S., Nielsen, E., Rietdorf, J. and Zerial, M. (2000). Distinct membrane domains on endosomes in the recycling pathway visualized by multicolor imaging of Rab4, Rab5, and Rab11. *J. Cell Biol.* **149**, 901-914.

Stoorvogel, W., Oorschot, V. and Geuze, H. J. (1996). A novel class of clathrin-coated vesicles budding from endosomes. *J. Cell Biol.* **132**, 21-33.

Traub, L. M. (2003). Sorting it out: AP-2 and alternate clathrin adaptors in endocytic cargo selection. *J. Cell Biol.* **163**, 203-208.

Ullrich, O., Reinsch, S., Urbe, S., Zerial, M. and Parton, R. G. (1996). Rab11 regulates recycling through the pericentriolar recycling endosome. *J. Cell Biol.* **135**, 913-924.

Wilcke, M., Johannes, L., Galli, T., Mayau, V., Goud, B. and Salamero, J. (2000). Rab11 regulates the compartmentalization of early endosomes required for efficient transport from early endosomes to the trans-Golgi network. *J. Cell Biol.* **151**, 1207-1220.

Wrigley, J. D., Ahmed, T., Nevett, C. L. and Findlay, J. B. C. (2000). Peripherin/rds influences membrane vesicle morphology. *J. Biol. Chem.* **275**, 13191-13194.

Wu, T. T. and Castle, J. D. (1997). Evidence for colocalization and interaction between 37 and 39 kDa isoforms of secretory carrier membrane proteins (SCAMPs). *J. Cell Sci.* **110**, 1533-1541.